

PAPER • OPEN ACCESS

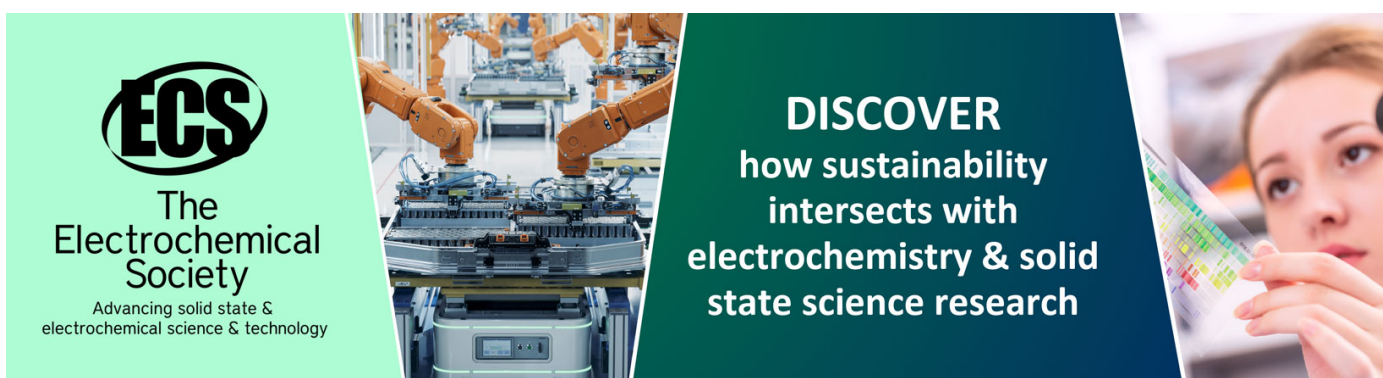
## Accuracy in evaluating convective heat transfer coefficient by RANS CFD simulations in a rectangular channel with high aspect ratio and 60° tilted staggered ribs

To cite this article: M Corti *et al* 2024 *J. Phys.: Conf. Ser.* **2685** 012001

View the [article online](#) for updates and enhancements.

You may also like

- [Turbulence closure modeling with data-driven techniques: physical compatibility and consistency considerations](#)  
Salar Taghizadeh, Freddie D Witherden and Sharath S Girimaji
- [BEYOND MIXING-LENGTH THEORY: A STEP TOWARD 321D](#)  
W. David Arnett, Casey Meakin, Maxime Viallet et al.
- [Tackling complex turbulent flows with transient RANS](#)  
Saša Kenjereš and Kemal Hanjali



**ECS**  
The  
Electrochemical  
Society  
Advancing solid state &  
electrochemical science & technology

**DISCOVER**  
how sustainability  
intersects with  
electrochemistry & solid  
state science research

# Accuracy in evaluating convective heat transfer coefficient by RANS CFD simulations in a rectangular channel with high aspect ratio and 60° tilted staggered ribs

M Corti<sup>1</sup>, P Gramazio<sup>1</sup>, D Fustinoni<sup>1</sup> and A Niro<sup>1,\*</sup>

<sup>1</sup> Politecnico di Milano, Department of Energy via Lambruschini 4, 20156 Milano, Italy

E-mail: \*alfonso.niro@polimi.it

**Abstract.** A numerical analysis of heat transfer characteristics of an air flow through a narrow rectangular channel of 1:10 aspect ratio with ribbed surfaces has been carried out, by means of a CFD commercial code, exploiting Reynolds Averaged Navier-Stokes (RANS) equations. The channel is 120 mm wide, 840 mm long, with 60° tilted staggered ribs. Ribs have a square cross section with two different side heights (2 mm and 4 mm) and three different values of dimensionless pitch (10, 20 and 40). The numerical results have been compared with experimental data obtained by the authors inside a ribbed channel both with same geometry and operating conditions as one numerically modelled. Agreement between numerical and experimental data on convective global heat transfer coefficient, i.e., averaged over the whole channel, is discussed for the six different configurations considered. Moreover, performances are presented by considering at the same time both heat transfer enhancement and pressure-drop penalization, highlighting strengths and weaknesses per each configuration. This work is aimed at finding a suitable configuration of a CFD model with RANS that will allow authors to apply it to the range of dimensionless pitches and side heights during early design-phases of parametric studies.

*Keywords:* forced convection, heat exchanger, rectangular channel, ribbed surfaces, experimental tests, CFD validation, RANS

## 1. Introduction

Considering the current and future scenario, aiming to reduce energy consumption and improve efficiency in the context of the green economy, heat transfer plays a significant role. In many engineering and electronic applications, innovative solutions are applied and studied to enhance heat transfer and increase efficiency. Regarding forced convection, this process has been largely studied in traditional fields like for the cooling of turbine blades [1] or for promoting heat transfer in nuclear reactors. In addition to



these well-established and extensively-studied areas, newer engineering applications have been lately investigated, like solar collectors [2] or more recently for automotive batteries cooling [3] and high-performance CPU cooling [4,5]. These novel industrial applications that require heat exchangers with large contact areas and very small heights can benefit from the use of ribs to enhance heat transfer associated to high aspect ratio rectangular channels with ribbed surfaces [6]. The result is more efficient and effective heat transfer, which can translate into significant energy savings and improved performance.

In literature, studies regarding former cases are quite extensive, although the documentation is somewhat fragmented or related to some specific application. Therefore, a systematic review has been conducted at Politecnico di Milano, over years, trying to establish general guidelines. Authors have conducted experimental analysis on fluid-dynamics and heat transfer characteristics of forced convection inside a ribbed channel with an aspect ratio of 1:10 [7], studying how varying ribs pitch-to-rib-side ratio, cross-section, or blockage ratio affects heat transfer. To reduce the experimental testing time, since CFD is a useful tool for studying fluid flow in ducts with rib roughened walls, authors have also developed CFD models using the RANS  $k - \omega - SST$  model, which has been widely used for similar cases compared to other RANS models given its effectiveness [8], and the LES model to achieve greater accuracy.

In this paper, results on convective heat transfer coefficient computed from RANS simulations are presented. The aim of this study is to continue with previous works and identify a suitable CFD model configuration, which can be applied to a range of ribs configurations.

## 2. Problem configuration and setup

### 2.1. Experimental setup

The experimental setup consists in a rectangular channel of 1:10 aspect ratio with 60° staggered ribs on the upper and the lower walls. Lower and upper walls of the experimental channel are kept at a fixed temperature, while the side walls and the ribs are adiabatic. The air flows at Reynolds number ranging from 700 to 8000, in this specific study Reynolds 7550 has been chosen. The experimental apparatus is described in details in [7] and the main geometric parameters are summarized in Table 1. Ribs analysed in this paper have a squared cross section, and a section side  $s$  of 2 mm and 4 mm. The ribs are 60° tilted with respect to the stream flow and staggered each other in each configuration proposed in this study. The pitch-to-side ratio  $p/s$  considered have been 10, 20, 40. For simplicity configurations considered will be named respectively P10S4, P20S4, P40S4 for ribs with width of 4 mm and P10S2, P20S2, and P40S2 for ribs with  $s=2$ mm. An overview of the channel can be seen in Figure 1a.

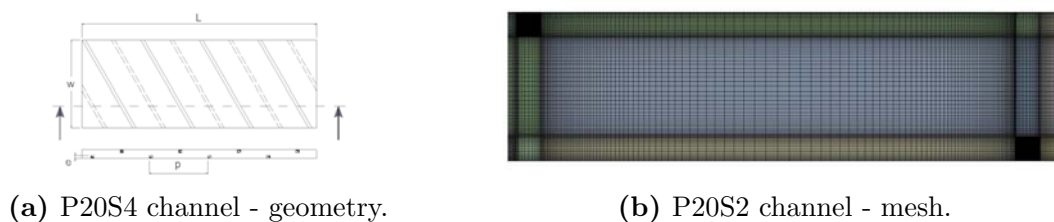
## 2.2. Numerical procedure

Numerical simulations have been carried out by means of a finite volume solver using the software Ansys Fluent 19.1. The solution domain consists in a 3D rectangular channel as described previously, to which two additional domains are merged: one dedicated to the entrance and one dedicated to the outlet. The latter is recommended to avoid reverse flows problems [9], frequent effects while dealing with geometries with obstacles such as ribs inside channels. The working fluid is air, incompressible, with negligible differences in specific heat at the temperatures considered.

The internal fluid flow has been analysed at  $Re$  7550, which is in a turbulent fluid flow regime. For this reason, the mesh adopted respects the parameters requested by the solver and by the problem, which will be introduced later. A sensitivity analysis has been carried out to obtain a grid independent solution analysing the three directions. It has been observed that the sensitivity to the mesh is greater in the  $y$ -direction or that in the direction of the channel height. Summarizing, several grids have been tested maintaining the same topology between them with a number of elements ranging from  $60 \cdot 10^6$  to  $100 \cdot 10^6$  and the grid finally chosen for the discretization of the examined geometries has about  $80 \cdot 10^6$  elements. Clearly the exact number varies based on the channel configuration. Using a medium quality mesh instead of a fine mesh leads in average to an error of 1% on the analysed parameters but in any case is lower than 4%. A sketch of the computational grid is shown in Figure 1b.

## 2.3. Boundary conditions

At the inlet of the computational domain a fully developed velocity profile, previously generated and based on the selected Reynolds number, is applied. The working fluid is air and it enters the channel at a uniform temperature, per example in most of the



(a) P20S4 channel - geometry.

(b) P20S2 channel - mesh.

**Figure 1.** Geometry and mesh overview.

**Table 1.** Main channel parameters.

Main geometric parameters	Value	Main geometric parameters	Value
Channel height, $2h=H$	12 mm	Ribs height, $e$	2 mm and 4 mm
Channel width, $2w=W$	120 mm	Ribs width, $s$	2 mm and 4 mm
Channel length, $L$	840 or 880 mm	Adimensional pitch $p/s$	$p/s=10, 20, 40$
Hydraulic diameter, $D_h$	21.28 mm	Reynolds number	7550

configuration is  $T_{in} = 296K$ . The temperature profile will develop inside the considered channel since the fluid flow is not thermally developed yet. At the outlet a pressure outlet with  $P_{out} = 0$  is applied. At walls a no-slip velocity condition is applied and all the walls (upper, lower and laterals) are maintained at a fixed constant temperature  $T_{wall} = 313.15K$ . Also walls of ribs have a no-slip velocity condition applied, but all of them are considered adiabatic, imposing  $q = 0$ . The choice to build adiabatic ribs is needed since authors want to highlight the beneficial effect of the ribs at a fluid-dynamic level, thus dissociating ribs from their possible fin behavior. The applied boundary conditions follow exactly the setup of the experimental apparatus with the exception of the boundary condition of the lateral walls. In the experimental setup they should be considered adiabatic while in the numerical model lateral walls are heated at a constant temperature. It has been seen through previous studies [10] that this boundary condition is the most suitable to ensure that the numerical problem best represents the experimental configuration.

#### 2.4. Solver settings and models

For pressure-velocity coupling the Semi-Implicit Method for Pressure Linked Equation-Consistent (SIMPLEC) segregated algorithm is used. This choice follows a comparison of other algorithms in previous trials showing a better and faster convergence, since in SIMPLEC algorithm the pressure-correction under-relaxation factor is generally set to 1.0. The gradients are discretized using a Least Squares Cell-Based scheme. The spatial discretization of pressure, momentum and energy equations is performed with a second order (upwind) scheme as for turbulent kinetic energy and specific dissipation rate. The flow has been solved with RANS, choosing the  $k - \omega - SST$  model. This choice has been motivated by evidence in literature [8] and by previous analysis [10].

The  $k - \omega - SST$  model uses as default the Enhanced Wall Treatment, requiring a careful sizing of the computational grid at walls that has to ensure a  $y^+ = 1$  at walls. Given the grid dimensions and the cores availability, in order to not exceed 96 hours of calculation per each single simulation, RANS simulations stop when the continuity residual is lower than  $1 \cdot 10^{-5}$ .

### 3. Results

In this study the air flow within the channels considered occurs at a Reynolds number equal to 7550. The choice of this Reynolds number is mainly due to two reasons. Firstly, it is currently the highest Reynolds number that has been tested experimentally with the current experimental setup, secondly, in agreement with previous analyses [10], it has been observed that using the RANS model  $k - \omega - SST$ , it improves its accuracy as the Reynolds number increases, considering  $Re > 5000$ .

Per each configuration considered, the heat transfer characteristics have been compared with the available experimental data that can be found in [7]. Values of

the friction factor and the average Nusselt number vs Reynolds number for staggered 60° tilted-ribs are presented in the reference [7] in Figure 6 and Figure 7, respectively. In the cited paper it's also possible to read about the error analysis and uncertainty that affects experimental data used as comparison in this work.

### 3.1. Bulk temperature and heat exchanged

Given the will to calibrate the numerical model on the experimental one, from experimental data is possible to directly compare the temperature measured at the outlet of the channel,  $T_{out}$ . The agreement is good because  $\Delta T_{experimental}/(T_{out} - T_{in})_{CFD} = 1.05$  although the percentage error remains lower than 1%. For this reason, the error on the thermal power could be representative. The heat exchanged  $Q$  by the air along the considered channel is calculated as  $Q = \dot{m}c_p(T_{out} - T_{in})$ , introducing some errors due to  $\dot{m}$ . Error remains lower than 5% for channel with ribs with  $s=4\text{mm}$  and ranges from 12% to 15% for channel with ribs with  $s=2\text{mm}$ . Figure 2 shows a summary of the data considered. Temperatures have been measured with a precision of  $0.05\text{K}$ , while the overall experimental uncertainty on  $Q$  is 2.3% calculated according to Moffat [11]. In the following figures the experimental uncertainties are represented by error bars.

### 3.2. Convective heat transfer coefficient

As usual approach, a conventional mean convective heat transfer coefficient is calculated from the energy balance as  $h_{m,ln} = \dot{m}c_p(T_{out} - T_{in})/(A\Delta T_{m,ln})$  when considering a channel with imposed wall temperature and a developed temperature profile. Comparing the mean convective heat transfer coefficients experimentally founded and numerically evaluated, the latter underestimate the experimental values, as can be seen in Figure 3a. Causes can be found in both the use of RANS model and the assumptions made since in the considered channels it is not certain that the temperature reaches the fully developed condition. Discrepancies increase while the channel complexity increases and

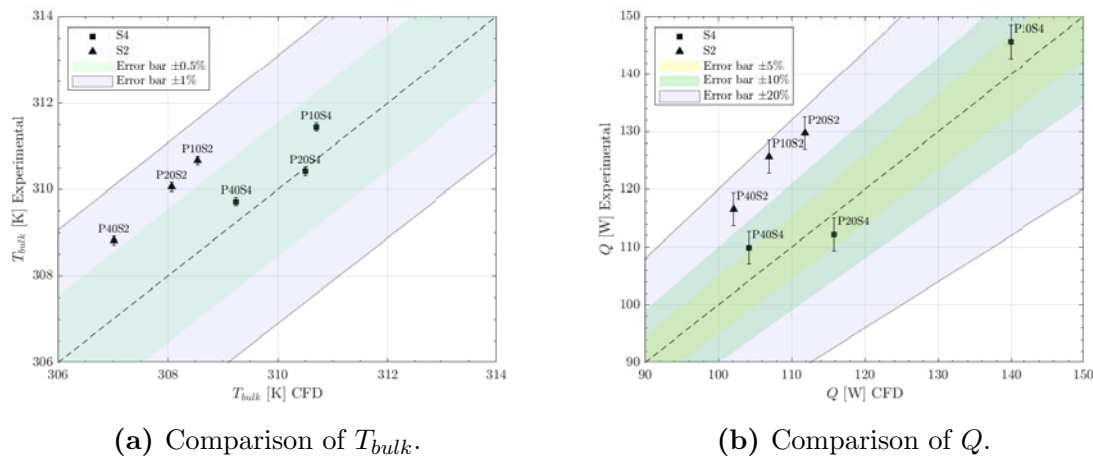


**Figure 2.** Comparison of experimental data versus CFD data,  $T_{bulk}$  and  $Q$ .

especially when rib height decreases, showing that the RANS model probably can not model correctly flow and heat transfer associated. The uncertainty associated to the experimental convective heat transfer coefficient is 3%.

Another quantity that can be analyzed, and that is interesting to propose, is the actual convective heat transfer coefficient,  $h_m$  (1), evaluated on the basis of numerical results.

$$h_m = \frac{1}{\sum_{z=1}^{n_{sections}} \Delta A_z} \left( \sum_{z=1}^{n_{sections}} h_z A_z \right) \quad (1)$$

Each contribution of the local convective heat transfer coefficient  $h_z$  has been weighed on the affected heat transfer surface  $\Delta A_z$  and sum up. This actual convective heat transfer coefficient provides a more comprehensive evaluation of the heat transfer coefficient with respect to  $h_{m,ln}$  since  $h_m$  considers also the effect of the channel entrance and the changes of  $h_z$  along the channel. To calculate the local heat transfer coefficient  $h_z$ , some sections, equidistant from each other, have been built along the channel length; an example of them can be seen in Figure 4a. The number of sections selected ensures that the actual convective heat transfer coefficient is no more influenced by the number of them. For each section the bulk temperature  $T_b$  and the heat flux  $q$  have been computed as mean section variables and mean line variables, respectively. Having this quantities, the local convective heat transfer coefficient can be computed at any sections as  $h_z = q_z / (T_w - T_{b,z})$ . Figure 4b shows the trend of the local convective heat transfer coefficient  $h_z$  plotted as a function of the length  $z$  of the channel. In the graph the trend of the  $h_z$  of a plane channel, without ribs, is also plotted as comparison. The presence of ribs shows a significant change in the trend for all configurations with  $s=4\text{mm}$ , whereas for 2 mm height ribs, when  $p/s$  is 10 and 20 a little change in the trend can be seen, but for the configuration P40S2 the trend is almost the same as the plane channel.

Lastly, comparing the values of  $h_{m,ln}$  and  $h_m$  in an area (downstream  $z=0.274\text{m}$ ) that could be considered far enough from entrance region, errors remain lower than 10% for channels with 4 mm height ribs, and lower than 5% for channels with rib height of 2 mm as can be seen in Table 2. This can be an indication on how much could be the error using  $h_{m,ln}$  instead of  $h_{m,z}$  for characterizing convective heat transfer coefficient in these channels.

**Table 2.** Comparison of convective heat transfer coefficient.

Channel Configuration	CFD $h_{m,ln}$ [ $W/m^2/K$ ]	CFD $h_{m,z}$ [ $W/m^2/K$ ] downstream $z=0.274\text{m}$	Error [-]
P10S4	101.69	92.68	9%
P20S4	85.05	77.81	9%
P40S4	64.20	61.07	5%
P10S2	64.55	61.29	5%
P20S2	59.10	57.56	3%
P40S2	48.63	46.54	4%

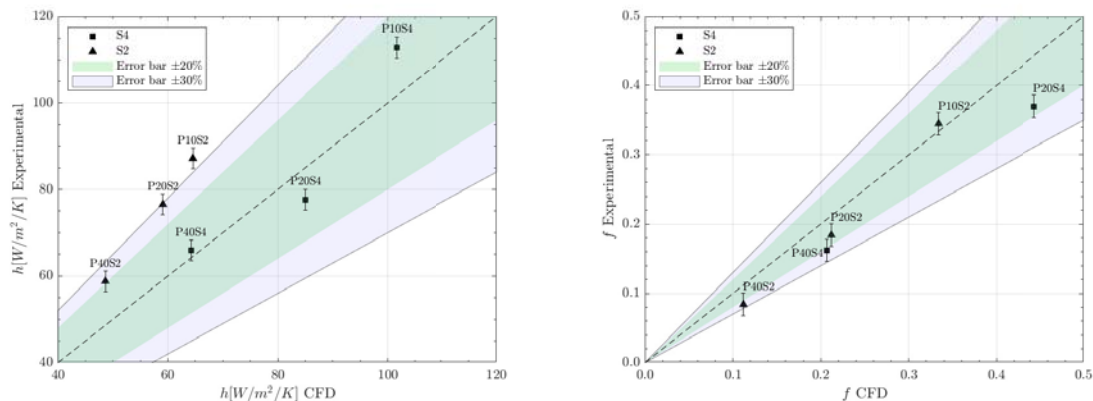
### 3.3. Pressure Drops

Friction factors  $f$  obtained from pressure drops  $\Delta P$ , deriving from numerical results through equation 2, have been compared with experimental data, measured with 7% uncertainty. Comparisons are shown in Figure 3b; notice that the experimental data of the configuration P10S4 is no available. Errors remain below the 5% for P10S2, below the 20% for P20S2 and P20S4 while for  $p/s=40$  errors are higher than 25%.

$$f = \frac{2\Delta P}{\rho u^2} \left( \frac{D_h}{L} \right) \quad (2)$$

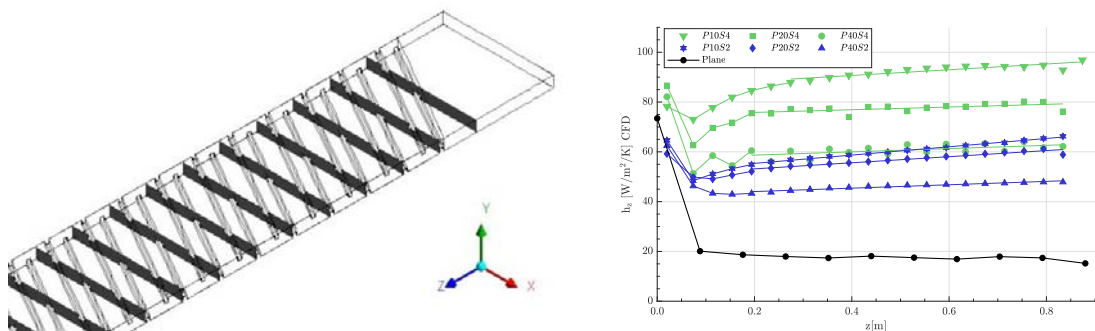
## 4. Discussion and Conclusions

In this study a CFD model has been developed for a rectangular channel with high aspect ratio and  $60^\circ$  tilted staggered ribs on upper and lower walls. The  $k - \omega - SST$  RANS model has been chosen and it has shown good agreement with experimental data at both fluid-dynamic and thermal levels. However, the increase in errors at lower ribs height could mean that RANS is not capable to capture with high accuracy the



(a) Comparison of heat transfer coefficient. (b) Comparison of friction factor coefficient.

**Figure 3.** Comparison of experimental data versus CFD data,  $h_{m,ln}$  and  $f$ .



(a) Exemplary section-planes. (b) Trend of the local heat transfer coefficient.

**Figure 4.** Local convective heat transfer coefficient, construction planes and trend.



swirling flows caused by little ribs. However, the reliability of  $k - \omega - SST$  model with respect to other RANS models, to Reynolds stress model, and to  $v^2 - f$  model has been proved in literature also for ribs with very small height, such as microribs with  $e/H \simeq 0.1$  [12]. The presented results are slightly less accurate than results presented in [13], where the ribs were  $90^\circ$  staggered, meaning that increasing the complexity of the channel RANS accuracy decreases. Nevertheless errors are acceptable, so this CFD model can be exploited as a starting point to expand the study of thermo-fluid dynamics of high aspect ratio channel with ribbed surfaces, limiting the need of experimental measurements. The intention is to build a database for some parametric studies or for the creation of correlations useful for the design-phase and the optimization of rib-roughened channels.

## References

- [1] Nourin F N and Amano R S Review of Gas Turbine Internal Cooling Improvement Technology 2021 *J. Energy Resour. Technol.* **143** 080801
- [2] Jain P K, Lanjewar A, Rana K B and Meena M L Effect of fabricated V-rib roughness experimentally investigated in a rectangular channel of solar air heater: a comprehensive review 2021 *Environ Sci Pollut Res* **28** 4019–4055
- [3] Huynh D and Mahjoob S 2020 Numerical Analysis of Structured Ribbed Channels for Electronic Cooling Applications 2020 *19th IEEE* pp 766–771
- [4] Zhao N, Guo L, Qi C, Chen T and Cui X Experimental study on thermo-hydraulic performance of nanofluids in CPU heat sink with rectangular grooves and cylindrical bugles based on exergy efficiency 2019 *Energy Convers. Manag.* **181** 235–246
- [5] Deng Z, Zhang S, Ma K, Jia C, Sun Y, Chen X, Luo Y, Li B and Li T Numerical and experimental study on cooling high power chips of data centers using double-side cooling module based on mini-channel heat sink 2023 *Appl. Therm. Eng.* **227** 120282
- [6] Bhattacharyya S, Vishwakarma D K, Srinivasan A, Soni M K, Goel V, Sharifpur M, Ahmadi M H, Issakhov A and Meyer J Thermal performance enhancement in heat exchangers using active and passive techniques: a detailed review 2022 *J Therm Anal Calorim* **147** 9229–9281
- [7] Fustinoni D, Gramazio P, Colombo L P M and Niro A First average and local heat transfer measurements on a forced air-flow at low Re-numbers through a rectangular channel with ribbed surfaces 2012 *J. Phys.: Conf. Ser.* **395** 012042
- [8] Sharma S K and Kalamkar V R Computational Fluid Dynamics approach in thermo-hydraulic analysis of flow in ducts with rib roughened walls – A review 2016 *Renew. Sust. Energ. Rev.* **55**
- [9] Pope S B 2000 *Turbulent Flows* 1st ed (Cambridge University Press)
- [10] Corti M, Gramazio P, Fustinoni D, Vitali L and Niro A Accuracy in evaluating heat transfer coefficient by RANS CFD simulations in a rectangular channel with high aspect ratio - Part 1: benchmark on a channel with plane walls 2023 *J. Phys.: Conf. Ser.* **2509** 012009
- [11] Moffat R J Describing the uncertainties in experimental results 1988 *Exp. Therm. Fluid Sci.* **1** 3–17
- [12] Li X, Zhang S, Zuo J, Wei J, Zhou X and Bao W Flow and heat transfer characteristics of supercritical hydrogen in unilateral heated channels with micro-ribs 2023 *Appl. Therm. Eng* **221** 119900
- [13] Corti M, Gramazio P, Fustinoni D, Vitali L and Niro A Accuracy in evaluating heat transfer coefficient by RANS CFD simulations in a rectangular channel with high aspect ratio - Part 2: channel with ribbed walls 2023 *J. Phys.: Conf. Ser.* **2509** 012010